

Skyrmions in the quantum Hall effect at finite Zeeman coupling.

A. G. Green, I. I. Kogan and A. M. Tsvelik

Department of Physics, University of Oxford, 1 Keble Road, Oxford OX1, UK

Using a self consistent approximation for the spin distribution of Skyrmions in the quantum Hall effect, we obtain an effective action for the Skyrmion coordinates. The energy functional is minimised for a periodic distribution of Skyrmions with an underlying hexagonal symmetry. We calculate the phonon spectrum of this lattice and find that near the classical minimum, breathing modes of the Skyrmions are strongly suppressed. The resulting equal sized Skyrmions interact via a residual Coulomb potential. Neglecting coupling between phonons and spin waves due to dipole and higher order Coulomb interactions, the Skyrmion crystal has a phonon spectrum identical to that of an electronic Wigner crystal. The transition to a liquid of equal sized Skyrmions is discussed using the theory of dislocation melting and a comparison is made between the predictions of this theory and the results of a recent experiment.

I. INTRODUCTION.

The theoretical prediction of Skyrmion spin textures in the fractional quantum Hall effect, made by Sondhi *et al.*¹, has prompted much theoretical work, supported by mounting experimental evidence, (see Refs. [2–4]).

Here, we consider the low temperature properties of a multi-Skyrmion system. Several parallel approaches have been developed to solve this problem. Historically, the first method, used in Ref.[1], employed a field theoretic description using a non-linear sigma model with a topological term. A solution for the partition function of topological excitations or Skyrmions in this model, in the absence of Zeeman and Coulomb interactions, was found by Fateev *et al.*⁵. At zero Zeeman energies and for sufficiently high temperature, this solution applies directly to the quantum Hall effect⁶ and describes a meron liquid. When the Zeeman energy is finite, the problem is complicated by the interplay between the Coulomb and Zeeman energies. As originally pointed out by Sondhi *et al.*¹, this fixes the scale for a single Skyrmion. In the multi-Skyrmion case, the problem is complicated further by the non-local nature of a Skyrmion spin distribution. The common belief, based on the analysis of a single Skyrmion, is that we have equal sized Skyrmions with some kind of residual interaction. We shall demonstrate that this belief is justified in the physically interesting range of parameters.

An alternative approach is to use a Hartree-Fock approximation⁷. In particular L. Brey *et al.* in Ref.[8] suggest that the zero temperature ground state of a multi-skyrmion system is a periodic structure rather like a Wigner crystal and pick out a face centred square lattice as the most stable of these. Our results, however, indicate that the ground state is closer to (or even perhaps, coincides with) a hexagonal structure.

Recently, a full microscopic quantum mechanical solution of the problem with a delta function interaction was presented by MacDonald *et al.*⁹. This approach requires computer diagonalization of the truncated Hamiltonian. It seems that it is rather difficult to apply this approach to systems with large numbers of Skyrmions.

In this paper we continue to develop the field theoretic description of the problem. In Section II, we introduce the energy functional and describe the Skyrmion solution. In Section III, we argue that for small Zeeman coupling the Skyrmions are only slightly distorted by the Coulomb and Zeeman interactions and are well approximated by the Belavin-Polyakov solutions¹⁰. We use this solution to investigate the experimentally relevant regime of Skyrmions of a small size. In Section V, we show that near the classical energy minimum the Skyrmions all have equal size and interact via a residual point-like Coulomb interaction. At low temperatures a Wigner crystal with rectangular symmetry is formed. We give an analytic expression for this structure and highlight its relationship to the square lattice predicted by Brey *et al.* and the hexagonal lattice expected for an electron Wigner crystal. In section VI, the phonon spectrum of the Skyrmion lattice is calculated followed by the spinwave spectrum in Section VII. In Section VIII, we discuss the dislocation mediated melting of the Skyrmion crystal to form a liquid of equal sized Skyrmions. The results of this analysis are compared with recent experiment. Finally in Section IX, we present a summary of our main results.

II. SKYRMIONS IN THE QUANTUM HALL EFFECT.

A. The Energy Functional.

In ref.[1], the following energy functional is suggested for the ferromagnetic order parameter in the fractional quantum Hall effect:

$$\begin{aligned} E &= E_{nl\sigma} + E_{Zeeman} + E_{Coulomb} \\ &= \int d^2x \left[\frac{\rho_s}{2} |\partial_\mu \mathbf{n}|^2 + \frac{\mu q}{\nu} - g_L \bar{\rho} B n^z \right] + \frac{1}{2} \int d^2x \int d^2x' q(r) V(r-r') q(r'), \end{aligned} \quad (1)$$

where, $\mathbf{n}(\mathbf{r})$ is an $O(3)$ order parameter for the spin, ρ_s is the spin stiffness, q the deviation in number density of electrons from uniform filling, $\bar{\rho}$ is the average density of electrons, ν the Landau level filling fraction, μ is a chemical potential for Skyrmions, and $V(\mathbf{r})$ is the Coulomb interaction potential. The filling fraction and average electron number density are related by, $\bar{\rho} = \nu/2\pi l^2$, where l is the magnetic length. Aside from the Coulomb interaction this is the usual continuous approximation for the energy of a ferromagnet. The Coulomb term arises because, in the quantum Hall effect, the electric charge density is proportional to the topological charge density¹:

$$q = -\frac{\nu}{8\pi} \epsilon_{\mu\nu} (\mathbf{n} \cdot [\partial_\mu \mathbf{n} \times \partial_\nu \mathbf{n}]). \quad (2)$$

B. Skyrmion Solution.

It is useful to parametrise the $O(3)$ field, $\mathbf{n}(\mathbf{r})$, as follows:

$$w = \frac{n_x + i n_y}{1 - n^z}, \quad n_x + i n_y = \frac{2w}{1 + |w|^2}, \quad n^z = \frac{|w|^2 - 1}{1 + |w|^2}. \quad (3)$$

Using this parameterisation of \mathbf{n} , the non-linear sigma part of the energy functional is,

$$E_{nl\sigma} = \int \frac{4d^2x}{(1 + |w|^2)^2} \left[\rho_s (|\partial w|^2 + |\bar{\partial} w|^2) - \frac{\mu}{4\pi} (|\partial w|^2 - |\bar{\partial} w|^2) \right], \quad (4)$$

where $z = x + iy$, $\partial = \partial/\partial z$ and $\bar{\partial} = \partial/\partial \bar{z}$. This is minimised on configurations called instantons or Skyrmions¹⁰, which have the form,

$$w(z) = h \prod_{i=1}^N \left(\frac{z - a_i}{z - b_i} \right), \quad (5)$$

where a_i, b_i, h are parameters. a_i and b_i are called the coordinates of the instanton. According to ref.[10], the energy of such a configuration is proportional to its topological charge, and does not depend on $\{h, a_i, b_i\}$: $E = (4\pi\rho_s - \mu)N$.

III. THE EFFECT OF COULOMB AND ZEEMAN INTERACTIONS.

A. Distortion of Skyrmions.

For a particular configuration of Skyrmions, the weak Zeeman and Coulomb interactions cause the spin distribution to distort slightly in order to minimise the energy. The energy of these distorted Skyrmions is not degenerate in their positions. The original distribution, $w = w_0$, becomes $w = w_0 + f$; $w_0(z)$ is analytic and $f(z, \bar{z})$ is some non-analytic function which we assume to be small compared with w_0 .

Expanding the variation of the non-linear sigma model part of the energy to first order in f , and using $Q_0 = \ln(1 + |w_0|^2)$ for ease of notation, we obtain,

$$\frac{\delta E_{nl\sigma}}{\delta w} = 8\rho_s [2w\partial\bar{w}\bar{\partial}\bar{w} - (1 + |w|^2)\partial\bar{\partial}\bar{w}]/(1 + |w|^2)^3 = -8\rho_s \bar{\partial}(e^{-2Q_0}\partial\bar{f}). \quad (6)$$

The total energy is minimised, that is $\frac{\delta E_{nl\sigma}}{\delta w} + \frac{\delta(E_{Coulomb} + E_{Zeeman})}{\delta w} = 0$, when,

$$\begin{aligned}
e^{-2Q_0} \partial \bar{f} &= \int^{\bar{z}} d\bar{\epsilon} \bar{w}_0(\bar{\epsilon}) G(w_0(z), \bar{w}_0(\bar{\epsilon})), \\
e^{-2Q_0} \bar{\partial} f &= \int^z d\epsilon w_0(\epsilon) G(w_0(\epsilon), \bar{w}_0(\bar{z})), \\
G(w(z), \bar{w}(\bar{z})) &= \frac{1}{8\rho_s} e^{-Q} \frac{\delta(E_{Coulomb} + E_{Zeeman})}{\delta Q}.
\end{aligned} \tag{7}$$

where $Q(\mathbf{x}) = \ln[1 + |w|^2(\mathbf{x})]$. The total energy is then,

$$E[w] = E_{nl\sigma}[w_0] + E_{z+c}[w_0] + E_{nl\sigma}^{ex}[w_0] + E_{z+c}^{ex}[w_0], \tag{8}$$

where,

$$\begin{aligned}
E_{nl\sigma}^{ex} &= 8\rho_s \int d^2x e^{-2Q} |\bar{\partial} f|^2, \\
E_{z+c}^{ex} &= \int d^2x e^{-Q} (w\bar{f} + \bar{w}f) \frac{\delta E_{z+c}}{\delta Q}.
\end{aligned} \tag{9}$$

By integrating by parts one may show that $E_{z+c}^{ex} = -2E_{nl\sigma}^{ex}$. From Eq.(7) we see that f is of order $g_L B/\rho_s$ and that the contributions to the total energy in Eq.(8) are of order ρ_s , $g_L B$ and $(g_L B)^2/\rho_s$ respectively.

Therefore, for small Zeeman coupling, $\rho_s \gg g_L B$, we may simply ignore these distortions (therefore from now on we shall drop the subscript 0), and minimise on the space of Skyrmion solutions given by Eq.(5). The energy functional with these approximations is,

$$\begin{aligned}
E &= (4\pi\rho_s - \mu)N + E_{Zeeman} + E_{Coulomb}, \\
E_{Zeeman} &= -g_L \bar{\rho} B \int d^2x (1 - 2e^{-Q}), \\
E_{Coulomb} &= \frac{1}{2} \left(\frac{e\nu}{4\pi}\right)^2 \int d^2x \int d^2x' 4\partial\bar{\partial}Q(1)V(\mathbf{x}_1 - \mathbf{x}_2)4\partial\bar{\partial}Q(2) \\
&= 8 \left(\frac{e\nu}{4\pi}\right)^2 \int d^2x_1 \int d^2x_2 \nabla_1^2 V(\mathbf{x}_1 - \mathbf{x}_2) Q(1)\partial\bar{\partial}Q(2).
\end{aligned} \tag{10}$$

In these expressions, $Q(1, 2) = Q(\mathbf{x}_{1,2})$ and the notation has been relaxed so that w now represents the undistorted Skyrmion spin distribution. We will use this convention from now on.

Taking the functional derivative of Eq.(10) with respect to w , we obtain the extremal condition,

$$g_L \bar{\rho} B e^{-Q} = \left(\frac{e\nu}{\pi}\right)^2 \int d^2x_2 \nabla_1^2 V(\mathbf{x}_1 - \mathbf{x}_2) \partial\bar{\partial}Q(2). \tag{11}$$

We have not been able to solve this equation analytically. It turns out, however, that for the experimentally relevant range of parameters we can come up with reasonable approximations.

IV. APPROXIMATING THE ENERGY FUNCTIONAL AND ITS DERIVATIVES.

A. The Energy Functional.

In order to make a useful approximation to the energy functional, we assume that the spin distribution is very sharply peaked around the zeros, a_i . This implies that the topological charge density at the zeros is much greater than the average charge density, which is in turn much greater than the charge density at the poles. That is, $q_{a_i} \gg \bar{q} \gg q_{b_i}$. Later, we will demonstrate the self-consistency of this approximation for the experimental range of parameters.

For spin distributions of this form, we may approximate the Coulomb and Zeeman energies by expanding w around its poles and zeros and integrating the corresponding approximate energy densities over patches around these points. The leading order behaviour of w near a pole or zero is,

$$\begin{aligned}
w(z \simeq a_i) &= \sqrt{\pi q_{a_i}} (z - a_i), \\
1/w(z \simeq b_i) &= \sqrt{\pi q_{b_i}} (z - b_i).
\end{aligned} \tag{12}$$

q_{a_i} and q_{b_i} are the topological charge densities at a_i and b_i , respectively:

$$\begin{aligned}\pi q_{a_i} &= \frac{|\partial w|^2}{(1+|w|^2)^2} = |\partial w(a_i)|^2 = |h|^2 \prod_{j=1, j \neq i}^N |a_i - a_j|^2 / \prod_{j=1}^N |a_i - b_j|^2, \\ \pi q_{b_i} &= \frac{|\partial(1/w)|^2}{(1+1/|w|^2)^2} = |\partial[w(a_i)]^{-1}|^2 = \frac{1}{|h|^2} \prod_{j=1, j \neq i}^N |b_i - b_j|^2 / \prod_{j=1}^N |b_i - a_j|^2.\end{aligned}\quad (13)$$

The variations of the topological charge density near a_i and b_i are,

$$\begin{aligned}\pi q(z \simeq a_i) &= \frac{\pi q_{a_i}}{(1 + \pi q_{a_i} |z - a_i|^2)^2}, \\ \pi q(z \simeq b_i) &= \frac{\pi q_{b_i}}{(1 + \pi q_{b_i} |z - b_i|^2)^2}.\end{aligned}\quad (14)$$

We are now in a position to approximate the Coulomb and Zeeman contributions to the energy functional. Firstly, the Zeeman energy is evaluated using the above approximations and integrating over circles of radius d centred on each a_i and b_i . πd^2 is the area per half Skyrmion and so $2\pi d^2$ is the area per Skyrmion. The radius d is related to the average Skyrmion density by,

$$\bar{q} = 1/2\pi d^2, \quad \bar{q} = |\nu/\nu_0 - 1|\bar{\rho}.\quad (15)$$

From Eq.(10), we find,

$$E_{Zeeman} = \frac{g\bar{\rho}B}{\bar{q}} \left(\sum_{a_i} 2\bar{q}/q_{a_i} \ln(1 + q_{a_i}/2\bar{q}) - \sum_{b_i} 2\bar{q}/q_{b_i} \ln(1 + q_{b_i}/2\bar{q}) \right).\quad (16)$$

Secondly, we evaluate the Coulomb energy. From Eq.(10) we find,

$$E_{Coulomb} = \frac{1}{2} \sum_i \left(\frac{e\nu}{\pi} \right)^2 \frac{\sqrt{\pi q_{a_i}}}{\epsilon} \underbrace{\int d^2 x_1 d^2 x_2 \frac{1}{(1+|x_1|^2)^2} \frac{1}{(1+|x_2|^2)^2}}_{\text{dimensionless constant} \sim O(1)} + \frac{1}{2} \sum_{i,j} \frac{(e\nu)^2}{\epsilon |a_i - a_j|}.\quad (17)$$

The first term is due to the local charge density at a_i and the second is an interaction between the charge densities near a_i and a_j . The latter has the form of a point particle interaction potential, since all the charge is concentrated in small regions of radius $1/\sqrt{\pi q_{a_i}}$ about a_i . The first term is dominant because, $q_{a_i} \gg \bar{q} \simeq 1/|a_i - a_j|^2$. Note that although the dominant contribution depends only upon the local density of charge, this local density depends on the Skyrmion coordinates in a non-local way, through q_{a_i} .

The total energy with these approximations is,

$$E = \frac{g\bar{\rho}B}{\bar{q}} \sum_i \left(2\bar{q}/q_{a_i} \ln(1 + q_{a_i}/2\bar{q}) - 2\bar{q}/q_{b_i} \ln(1 + q_{b_i}/2\bar{q}) + 2\alpha \sqrt{q_{a_i}/2\bar{q}} \right) + \frac{1}{2} \sum_{i,j} \frac{(e\nu)^2}{\epsilon |a_i - a_j|},\quad (18)$$

where,

$$\alpha = \frac{\bar{q}}{g_L \bar{\rho} B} \left(\frac{e\nu}{2\pi} \right)^2 \frac{\sqrt{2\pi\bar{q}}}{\epsilon} = \frac{\nu_0 |\nu/\nu_0 - 1|^{3/2}}{(2\pi)^2} \frac{e^2}{\epsilon l g_L B} \approx (0.4 \rightarrow 1.6) \nu_0 |\nu/\nu_0 - 1|^{3/2}.\quad (19)$$

In final expression, we have substituted the typical experimental values of the ratio $g_L B \epsilon l / e^2 \approx 0.01 \rightarrow 0.04^{2-4}$.

B. Derivatives of the Energy Functional.

In order to determine the minimal Skyrmion configuration and its stability, we require the first and second derivatives of the energy functional with respect to the Skyrmion positions. These may be approximated by evaluating the derivative of the total energy, Eq.(10), and expanding the resulting integrals as in the preceding Section. The derivative of the energy with respect to the position of a pole or zero, r_i , is

$$\begin{aligned} \frac{\partial E}{\partial r_i} = & \pm \frac{g\bar{\rho}B}{\bar{q}} \sum_k \left(2\bar{q}/q_{a_k} \ln(1 + q_{a_k}/2\bar{q}) - (1 + q_{a_k}/2\bar{q})^{-1} - \alpha\sqrt{q_{a_k}/2\bar{q}} \right) / (a_k - r_j) \\ & \pm \frac{g\bar{\rho}B}{\bar{q}} \sum_i \left(2\bar{q}/q_{b_k} \ln(1 + q_{b_k}/2\bar{q}) - (1 + q_{b_k}/2\bar{q})^{-1} \right) / (b_k - r_j). \end{aligned} \quad (20)$$

The plus/minus sign is taken when r_i corresponds to a zero/pole. The second derivatives are given by,

$$\begin{aligned} \frac{\partial^2 E}{\partial r_i \partial s_j} = & \pm \frac{g\bar{\rho}B}{\bar{q}} \sum_k \left(2\bar{q}/q_{a_k} \ln(1 + q_{a_k}/2\bar{q}) + (1 + q_{a_k}/\bar{q})(1 + q_{a_k}/2\bar{q})^{-1} + 1/2\alpha\sqrt{q_{a_k}/2\bar{q}} \right) / (a_k - r_i)(a_k - s_j) \\ & \pm \frac{g\bar{\rho}B}{\bar{q}} \sum_k \left(-2\bar{q}/q_{b_k} \ln(1 + q_{b_k}/2\bar{q}) + (1 + q_{b_k}/\bar{q})(1 + q_{b_k}/2\bar{q})^{-1} \right) / (b_k - r_i)(b_k - s_j), \end{aligned} \quad (21)$$

where the plus sign is taken when both r_i and s_j correspond to a pole or zero and the minus sign otherwise. For the present we have ignored the contribution from the residual Coulomb interaction. This will be reintroduced later.

V. THE CLASSICAL MINIMUM.

The classical minimum is attained when the derivative of the energy is zero with respect to all of the Skyrmion coordinates. From Eq.(20), this occurs when, to logarithmic accuracy,

$$q_{a_i} = q_0 = 2\bar{q} \left(\frac{-2 \ln \alpha}{3\alpha} \right)^{2/3}, \quad q_{b_i} \simeq 0, \quad \forall_i. \quad (22)$$

As we have already mentioned, our approximation requires $q_0 \gg \bar{q}$ which according to Eq.(19) is achieved for a deviation of ν from ν_0 of less than 0.2 ($q_0/\bar{q} \approx 5 \rightarrow 20$ for experimental values of $g_L B \ell / e^2 \approx 0.01 \rightarrow 0.04$ and $|\nu/\nu_0 - 1| = 0.2$).

Eq.(22) gives $2N$ constraints on the values of q_{a_i} and q_{b_i} , and so constrains the positions, a_i, b_i . For any particular arrangement of a_i , we may satisfy the above constraint by fixing b_i . The number of degrees of freedom is reduced by a factor of two. At the classical minimum the intuitive picture holds. Equal sized Skyrmions with $w = z/r_0$, matched to the ferromagnetic background, move independently except for the residual Coulomb interaction given by the second term in Eq.(17). In the single Skyrmion sector, this is the result of Sondhi *et al.*¹.

At low enough temperatures Skyrmions interacting in this way are expected to form a classical Wigner crystal. The calculation of Bonsall *et al.*¹², performed for an electronic Wigner crystal, suggests a hexagonal lattice as the minimal solution. We argue that the same calculation is valid for the crystal of Skyrmions. This brings us into disagreement with the results of Ref.[8]. However, this is 'simply' because these authors did not consider a hexagonal lattice of the proper type. The simplest periodic arrangement of Skyrmions is described by a bi-periodic analytic (elliptic) function, w , with two poles and two zeros per unit cell; b, b' and a, a' respectively. A general property of such an elliptic function is that $|w(z - a)|^2 = |w(z - a')|^2$ and $|w(z - b)|^2 = |w(z - b')|^2$. The dependence of the energy functional on $|w|^2$ and so n^z alone, allows us to treat a and a' , (and also b and b'), on an equal footing. The Wigner lattices have a 's and a' 's on alternate lattice sites. The hexagonal lattice predicted here, therefore, is not the higher energy hexagonal lattice investigated by L. Brey *et al.*, but rather a distortion of their face centred square lattice to a face centred rectangular lattice with sides in the ratio $1 : \sqrt{3}$. Figures 1 and 2 show the azimuthal components of the spin distributions corresponding to the face centred square and face centred rectangular lattice. Analytic expressions for these are given by Jacobi elliptic functions; $w = h \operatorname{cn}(z, 1/\sqrt{2})$ for the square lattice and $w = h \operatorname{cn}(z, e^{i2\pi/3})$ for the hexagonal/rectangular lattice. Since our analysis has neglected dipole and higher moments of the charge distribution, the real structure is likely to be a rectangular lattice with the ratio of sides close to $1 : \sqrt{3}$.

To be sure of this result, we must investigate its stability by evaluating the phonon spectrum. In addition to the usual phonon modes of the Wigner crystal there will be modes corresponding to fluctuations in the size of the Skyrmions and to spinwaves.

VI. PHONON SPECTRUM OF THE SKYRME CRYSTAL.

A. The Wigner crystal.

Here we present in condensed form the results of Bonsall *et al.* for the normal modes of a classical Wigner crystal. The residual coulomb interaction is,

$$E = \frac{1}{2} \sum_{i,j} \frac{(e\nu)^2}{\epsilon |a_i - a_j|}, \quad (23)$$

and its derivatives with respect to the positions of the Skyrmions are,

$$\begin{aligned} \frac{\partial^2 E}{\partial a_i \partial a_j} &= -\frac{3(e\nu)^2}{4\epsilon} \frac{\bar{a}_{ij}^2}{|a_{ij}|^5}, \quad \frac{\partial^2 E}{\partial a_i \partial a_i} = +\frac{3(e\nu)^2}{4\epsilon} \sum_{j \neq i} \frac{\bar{a}_{ij}^2}{|a_{ij}|^5}, \\ \frac{\partial^2 E}{\partial a_i \partial \bar{a}_j} &= -\frac{(e\nu)^2}{4\epsilon} \frac{1}{|a_{ij}|^3}, \quad \frac{\partial^2 E}{\partial a_i \partial \bar{a}_i} = +\frac{(e\nu)^2}{4\epsilon} \sum_{j \neq i} \frac{1}{|a_{ij}|^3}. \end{aligned}$$

These are Fourier transformed to give the dynamical matrix,

$$\begin{aligned} \tilde{D}_{aa}(k) &= \frac{\pi(e\nu)^2}{2\epsilon} \frac{\bar{k}^2}{|k|}, \\ \tilde{D}_{a\bar{a}}(k) &= \frac{\pi(e\nu)^2}{2\epsilon} |k|, \\ D_{rs}(k) &= \frac{1}{V_c} \sum_{\mathbf{G}} \tilde{D}_{rs}(k), \end{aligned} \quad (24)$$

where \mathbf{G} is a reciprocal lattice vector. To evaluate the normal modes one must first recast these summations into a more rapidly convergent form, Ref.[12]. The result for the hexagonal crystal, written in terms of the longitudinal and transverse components, $r, s \in \{a_L, a_T, \}$, is,

$$D_{rs}^{Wigner} = \begin{pmatrix} \mathcal{L}(|\mathbf{k}| - 0.181a_0|\mathbf{k}|^2) & 0 \\ 0 & \mathcal{T}|\mathbf{k}|^2 \end{pmatrix}, \quad \mathcal{L} = \frac{2\pi(e\nu)^2}{\epsilon V_c}, \quad \mathcal{T} = \frac{2\pi(e\nu)^2}{\epsilon V_c} 0.036a_0. \quad (25)$$

a_0 is the lattice spacing and V_c is the area of a unit cell.

B. Contribution of Non-Local Terms.

For a periodic lattice at the classical minimum, the second derivatives of the nonlocal part of the energy functional (21) are given by,

$$\frac{\partial^2 E}{\partial r_i \partial \bar{s}_j} = \pm \left(\frac{e\nu}{2\pi} \right)^2 \frac{3\sqrt{\pi q_0}}{2\epsilon} \sum_{a_k \neq r_i, s_j} \frac{1}{(a_k - r_i)(\bar{a}_k - \bar{s}_j)} \quad (26)$$

Terms like $\partial^2 E / \partial a_i \partial a_j$ are zero for a periodic lattice. Taking the Fourier transform of these derivatives, we obtain the elements of the dynamical matrix,

$$\begin{aligned} D_{a\bar{a}} &= 3(e\nu)^2 \frac{\sqrt{\pi q_0}}{2\epsilon V_c} \sum_{\mathbf{G}\mathbf{G}'} \left(\frac{1}{(k+G)(\bar{k}+\bar{G}')} - \frac{1}{(k+G)\bar{G}'} - \frac{1}{G(\bar{k}+\bar{G}')} + \frac{1}{G\bar{G}'} \right), \\ D_{a\bar{b}} &= - \quad " \quad \sum_{\mathbf{G}\mathbf{G}'} \left(\frac{e^{-i\mathbf{G}\cdot\mathbf{b}}}{(k+G)(\bar{k}+\bar{G}')} - \frac{e^{-i\mathbf{G}\cdot\mathbf{b}}}{(k+G)\bar{G}'} \right), \\ D_{b\bar{a}} &= - \quad " \quad \sum_{\mathbf{G}\mathbf{G}'} \left(\frac{e^{-i\mathbf{G}\cdot\mathbf{b}}}{(k+G)(\bar{k}+\bar{G}')} - \frac{e^{-i\mathbf{G}\cdot\mathbf{b}}}{(k+G)\bar{G}'} \right), \\ D_{b\bar{b}} &= \quad " \quad \sum_{\mathbf{G}\mathbf{G}'} \left(\frac{e^{-i\mathbf{G}\cdot\mathbf{b}}}{(k+G)} \frac{e^{+i\mathbf{G}\cdot\mathbf{b}}}{(\bar{k}+\bar{G}')} \right). \end{aligned} \quad (27)$$

The summations over the reciprocal lattice vectors, \mathbf{G} and \mathbf{G}' , are only very slowly convergent and must be re-cast into a more rapidly convergent form. In order to do this, we use a modification of the Ewald separation method, (see refs.[11] and [12]). This involves splitting a slowly convergent real lattice sum into summations over the real lattice and the reciprocal lattice, both of which are rapidly convergent. Firstly, we write the elements of the dynamical matrix in the following way:

$$D_{a\bar{a}}(\mathbf{k}) = - \left(\frac{e\nu}{2\pi} \right)^2 \frac{3\sqrt{\pi q_0}}{2\epsilon} \left(\sum_{\mathbf{a}_l \neq 0} \frac{e^{i\mathbf{k} \cdot \mathbf{a}_l}}{a_l} \right) \left(\sum_{\mathbf{a}_l \neq 0} \frac{e^{i\mathbf{k} \cdot \mathbf{a}_l}}{\bar{a}_l} \right), \quad (28)$$

$$D_{a\bar{b}}(\mathbf{k}) = + \left(\frac{e\nu}{2\pi} \right)^2 \frac{3\sqrt{\pi q_0}}{2\epsilon} \left(\sum_{\mathbf{a}_l \neq 0} \frac{e^{i\mathbf{k} \cdot \mathbf{a}_l}}{a_l} \right) \left(\sum_{\mathbf{a}_l} \frac{e^{i\mathbf{k} \cdot (\mathbf{a}_l - \mathbf{b})}}{\bar{a}_l - \bar{b}} \right), \quad (29)$$

$$D_{b\bar{a}}(\mathbf{k}) = + \left(\frac{e\nu}{2\pi} \right)^2 \frac{3\sqrt{\pi q_0}}{2\epsilon} \left(\sum_{\mathbf{a}_l} \frac{e^{i\mathbf{k} \cdot (\mathbf{a}_l + \mathbf{b})}}{a_l + b} \right) \left(\sum_{\mathbf{a}_l \neq 0} \frac{e^{i\mathbf{k} \cdot \mathbf{a}_l}}{\bar{a}_l} \right), \quad (30)$$

$$D_{b\bar{b}}(\mathbf{k}) = - \left(\frac{e\nu}{2\pi} \right)^2 \frac{3\sqrt{\pi q_0}}{2\epsilon} \left(\sum_{\mathbf{a}_l} \frac{e^{i\mathbf{k} \cdot (\mathbf{a}_l + \mathbf{b})}}{a_l + b} \right) \left(\sum_{\mathbf{a}_l} \frac{e^{i\mathbf{k} \cdot (\mathbf{a}_l - \mathbf{b})}}{\bar{a}_l - \bar{b}} \right). \quad (31)$$

Next, using the integral representation,

$$\frac{1}{|\mathbf{x}|^2} = \int_0^\infty dt e^{-t|\mathbf{x}|^2}, \quad (32)$$

and the two dimensional theta-function transformation,

$$\sum_{\mathbf{a}_l} \exp \{ -t|\mathbf{x} - \mathbf{a}_l|^2 + i\mathbf{k} \cdot \mathbf{a}_l \} = \frac{\pi}{V_c t} \sum_{\mathbf{G}} \exp \{ -|\mathbf{G} - \mathbf{k}|^2/4t - i\mathbf{G} \cdot \mathbf{x} \}, \quad (33)$$

we consider the lattice sums,

$$\sum_{\mathbf{a}_l \neq 0} \frac{e^{i\mathbf{k} \cdot \mathbf{a}_l}}{|\mathbf{a}_l|^2} = \sum_{\mathbf{a}_l \neq 0} \int_\gamma^\infty dt e^{-t|\mathbf{a}_l|^2 + i\mathbf{k} \cdot \mathbf{a}_l} + \sum_{\mathbf{G}} \frac{\pi}{V_c} \int_0^\gamma \frac{dt}{t} e^{-|\mathbf{G} - \mathbf{k}|^2/4t} - \lim_{x \rightarrow 0} \int_0^\gamma dt e^{-t|\mathbf{x}|^2 + i\mathbf{k} \cdot \mathbf{x}} \quad (34)$$

$$\sum_{\mathbf{a}_l} \frac{e^{i\mathbf{k} \cdot (\mathbf{a}_l \pm \mathbf{b})}}{|\mathbf{a}_l \pm \mathbf{b}|^2} = \sum_{\mathbf{a}_l} \int_\gamma^\infty dt e^{-t|\mathbf{a}_l \pm \mathbf{b}|^2 + i\mathbf{k} \cdot (\mathbf{a}_l \pm \mathbf{b})} + \sum_{\mathbf{G}} \frac{\pi}{V_c} \int_0^\gamma \frac{dt}{t} e^{-|\mathbf{G} - \mathbf{k}|^2/4t \mp i(\mathbf{G} + \mathbf{k}) \cdot \mathbf{b}}. \quad (35)$$

In these expressions, $V_c = \bar{q}^{-1}$ is the area of a unit cell and γ is the Ewald separation parameter. The result is independent of the value of γ , which is chosen so that both the lattice and reciprocal lattice summations on the right hand side are rapidly convergent. For small wave-vector, \mathbf{k} , the $\mathbf{G} = 0$ term dominates;

$$\begin{aligned} \sum_{\mathbf{a}_l \neq 0} \frac{e^{i\mathbf{k} \cdot \mathbf{a}_l}}{|\mathbf{a}_l|^2} &= \frac{\pi}{V_c} (-\text{constant} - \ln(|\mathbf{k}|^2/4\gamma)), \\ \sum_{\mathbf{a}_l} \frac{e^{i\mathbf{k} \cdot (\mathbf{a}_l \pm \mathbf{b})}}{|\mathbf{a}_l \pm \mathbf{b}|^2} &= \frac{\pi \cos(\mathbf{k} \cdot \mathbf{b})}{V_c} (-\text{constant} - \ln(|\mathbf{k}|^2/4\gamma)). \end{aligned} \quad (36)$$

We have used the fact that since \mathbf{b} lies at the centre of the unit cell, the second summation is independent of its sign. Finally, we differentiate with respect to $k = k_x + ik_y$ to obtain,

$$\begin{aligned} \sum_{\mathbf{a}_l \neq 0} \frac{e^{i\mathbf{k} \cdot \mathbf{a}_l}}{a_l} &= -2i \frac{\partial}{\partial k} \sum_{\mathbf{a}_l \neq 0} \frac{e^{i\mathbf{k} \cdot \mathbf{a}_l}}{|\mathbf{a}_l|^2} = \frac{2\pi i}{V_c} \frac{1}{k}, \\ \sum_{\mathbf{a}_l} \frac{e^{i\mathbf{k} \cdot \mathbf{a}_l}}{a_l \pm b} &= -e^{\mp i\mathbf{k} \cdot \mathbf{b}} 2i \frac{\partial}{\partial k} \sum_{\mathbf{a}_l} \frac{e^{i\mathbf{k} \cdot (\mathbf{a}_l \pm \mathbf{b})}}{|\mathbf{a}_l \pm \mathbf{b}|^2} = \frac{2\pi i}{V_c} \frac{e^{\mp i\mathbf{k} \cdot \mathbf{a}}}{k}. \end{aligned} \quad (37)$$

Substituting for these expressions into Eqs.(28) to (31), the contribution to the dynamical matrix from the non-local interaction is,

$$D_{rs}^{non-Local} = \begin{pmatrix} 0 & 0 & 1 & -e^{i\mathbf{k}\cdot\mathbf{b}} \\ 0 & 0 & -e^{-i\mathbf{k}\cdot\mathbf{b}} & 1 \\ 1 & -e^{i\mathbf{k}\cdot\mathbf{b}} & 0 & 0 \\ -e^{-i\mathbf{k}\cdot\mathbf{b}} & 1 & 0 & 0 \end{pmatrix} \delta/|\mathbf{k}|^2, \quad (38)$$

where,

$$\delta = 3\bar{q}^2 (e\nu)^2 \frac{\sqrt{\pi q_0}}{2\epsilon}. \quad (39)$$

This does not depend upon the lattice type. The interaction is so long range that it is insensitive to the small scale distribution of the Skyrmions. In fact our final result is just that obtained using a continuous Fourier transform of the derivatives.

C. Phonon Spectrum of the Skyrmion Crystal.

To determine the spectrum of the Skyrme crystal, we require the eigen-modes of the total dynamical matrix, $D_{rs}^{Wigner} + D_{rs}^{non-Local}$. We will concentrate on the hexagonal lattice, since this is the minimum energy at our level of approximation. In terms of the longitudinal and transverse components, $r, s \in \{a_L, b_L, a_T, b_T\}$, the dynamical matrix is,

$$D_{rs} = \begin{pmatrix} \mathcal{L}|\mathbf{k}| & 0 & 0 & 0 \\ 0 & 0 & 0 & 0 \\ 0 & 0 & \mathcal{T}|\mathbf{k}|^2 & 0 \\ 0 & 0 & 0 & 0 \end{pmatrix} + \begin{pmatrix} 1 & -e^{i\mathbf{k}\cdot\mathbf{b}} & 0 & 0 \\ -e^{-i\mathbf{k}\cdot\mathbf{b}} & 1 & 0 & 0 \\ 0 & 0 & 1 & -e^{i\mathbf{k}\cdot\mathbf{b}} \\ 0 & 0 & -e^{-i\mathbf{k}\cdot\mathbf{b}} & 1 \end{pmatrix} 2\delta/|\mathbf{k}|^2 \quad (40)$$

The first matrix is given by Eq.(25). The second matrix is obtained from Eq.(38) by multiplying on the left and right by matrices Λ^T and Λ respectively, such that,

$$\begin{pmatrix} a_L \\ b_L \\ a_T \\ b_T \end{pmatrix} = \underbrace{\frac{1}{2|\mathbf{k}|} \begin{pmatrix} k_x & 0 & k_y & 0 \\ 0 & k_x & 0 & k_y \\ k_y & 0 & -k_x & 0 \\ 0 & k_y & 0 & -k_x \end{pmatrix} \begin{pmatrix} 1 & 0 & 1 & 0 \\ 0 & 1 & 0 & 1 \\ -i & 0 & i & 0 \\ 0 & -i & 0 & i \end{pmatrix}}_{\Lambda^{-1}} \begin{pmatrix} a \\ b \\ \bar{a} \\ \bar{b} \end{pmatrix} \quad (41)$$

The problem separates into two independent sectors. In the longitudinal sector, the eigen values and eigen-vectors for small wave-vector are,

$$\mathcal{L}|\mathbf{k}|/2, \begin{pmatrix} 1 \\ e^{-i\mathbf{k}\cdot\mathbf{b}} \end{pmatrix} \text{ and } 4\delta/|\mathbf{k}|^2, \begin{pmatrix} 1 \\ -e^{-i\mathbf{k}\cdot\mathbf{b}} \end{pmatrix}. \quad (42)$$

In the transverse sector the eigen-modes are,

$$\mathcal{T}|\mathbf{k}|^2/2, \begin{pmatrix} 1 \\ e^{-i\mathbf{k}\cdot\mathbf{b}} \end{pmatrix} \text{ and } 4\delta/|\mathbf{k}|^2, \begin{pmatrix} 1 \\ -e^{-i\mathbf{k}\cdot\mathbf{b}} \end{pmatrix}. \quad (43)$$

The $1/|\mathbf{k}|^2$ modes are extremely stiff, and basically ensure that at finite Zeeman coupling the Skyrmions have a fixed size. Note, however, that according to Eq.(39) $\delta \propto (g_L \ln g_L)^{1/3}$ and so at zero Zeeman energy we expect substantial variation in the size. The remaining modes are the usual Wigner crystal modes.

D. Quantum Fluctuations of Phonons.

The above calculation of the derivatives of the energy functional describes the properties of the Skyrmion crystal in regimes where the quantum fluctuations may be neglected. We require a full quantum treatment of the phonon spectrum. The dynamical part of the action for Skyrmions in the quantum Hall effect is given by the Wess-Zumino term,

$$S_{WZ} = \frac{\nu\bar{\rho}}{2} \int d^2x dt \mathbf{A}[\mathbf{n}(\mathbf{r})] \cdot \frac{\partial \mathbf{n}}{\partial t} = \frac{\nu\bar{\rho}}{2} \int d^2x dt d\tau \mathbf{n} \cdot (\partial_t \mathbf{n} \times \partial_\tau \mathbf{n}) = 2\nu\bar{\rho} \int d^2x dt d\tau \frac{|\partial_T w|^2 - |\bar{\partial}_T w|^2}{(1 + |w|^2)^2}, \quad (44)$$

where $T = t + i\tau$, $\partial_T = \partial/\partial T$ and $\bar{\partial}_T = \partial/\partial \bar{T}$. We have extended the function $\mathbf{n}(t)$ to a function $\mathbf{n}(t, \tau)$ in the usual way, such that t and $0 \leq \tau \leq 1$ parameterise the interior of the region bounded by the curve $\mathbf{n}(t)$ with $\mathbf{n}(t, 1) = \mathbf{n}(t)$ ¹⁷. This puts the action into a manifestly gauge invariant form. The third expression is obtained by substitution of the linear map, Eq.(3), into this gauge invariant form.

We may approximate this contribution to the action in the same way as the energy functional, by assuming that the spin distribution is sharply peaked around the zeros, a_i . Integrating over patches around these points we obtain,

$$\begin{aligned} S_{WZ} &= 2\nu\bar{\rho} \int d^2x dt d\tau \sum_i (|\partial_T a_i|^2 - |\bar{\partial}_T a_i|^2) \pi q_{a_i}(\mathbf{x}) \\ &= 2\pi\nu\bar{\rho} \sum_i \int dt d\tau (|\partial_T a_i|^2 - |\bar{\partial}_T a_i|^2) \\ &= -2\pi\nu\bar{\rho} \sum_i \int dt d\tau (\partial_\tau a_{i,x} \partial_t a_{i,y} - \partial_\tau a_{i,y} \partial_t a_{i,x}) \\ &= -\pi\nu\bar{\rho} \sum_i \int dt (a_{i,x} \partial_t a_{i,y} - a_{i,y} \partial_t a_{i,x}) \\ &= \pi\nu\bar{\rho} \sum_i \int dt \mathbf{a}_i \epsilon \partial_t \mathbf{a}_i, \end{aligned} \quad (45)$$

where ϵ is the two dimensional anti-symmetric tensor,

$$\epsilon = \begin{pmatrix} 0 & -1 \\ 1 & 0 \end{pmatrix}. \quad (46)$$

This is simply the result presented by M. Stone¹⁴ for the single Skyrmion and is the Lorentz force for a particle of unit charge moving in a magnetic field $2\pi\nu\bar{\rho} = e\nu^2 B$. Combining this with the approximation to the energy functional made above, we obtain an effective action for the phonon modes of the Skyrmion crystal as follows:

$$S_{eff} = \frac{1}{2} \sum_{\omega} \int \frac{d^2k}{(2\pi)^2} \delta \mathbf{a}(\omega, -\mathbf{k}) (i\omega e\nu^2 B \epsilon - D(\mathbf{k})) \delta \mathbf{a}(\omega, \mathbf{k}). \quad (47)$$

Since we are only interested in phonon modes which do not change the size of the Skyrmions, we retain only the corresponding elements of D_{rs} . Therefore, $D(\mathbf{k})$ is the two by two matrix $D_{rs}^{Wigner}/2$ given by Eq.(25). The equation of motion for these fluctuations is

$$(i\omega e\nu^2 B \epsilon - D(\mathbf{k})) \delta \mathbf{a}(\omega, \mathbf{k}) = 0. \quad (48)$$

If we follow Refs.[14,15] and introduce a kinetic term, $m^* |\partial_t \mathbf{n}|^2/2$, into the Lagrangian, the equation of motion becomes,

$$(\omega^2 m^* + i\omega e\nu^2 B \epsilon - D(\mathbf{k})) \delta \mathbf{a}(\omega, \mathbf{k}) = 0. \quad (49)$$

Substituting explicit expressions for the matrix $D(\mathbf{k})$ from Eq.(25) we find that the frequencies of the longitudinal and transverse modes are,

$$\begin{aligned} \omega_t &= \frac{\sqrt{\mathcal{L}\mathcal{T}}}{2\omega_c m^*} |\mathbf{k}|^{3/2}, \\ \omega_l &= \omega_c = \frac{eB}{m^* c}. \end{aligned} \quad (50)$$

This is identical to the result for an electronic Wigner crystal in a magnetic field given in Ref.[13].

VII. SPIN WAVES IN THE SKYRMION CRYSTAL.

The analysis up to now has been concerned with finding the groundstate spin distribution. We have argued that this is a slightly distorted version of the Belavin-Polyakov Skymion solution and have minimised the energy functional on the space of these solutions. When considering the dynamical properties of the system one must include the possibility of spin waves. These have been excluded up to now for a fundamental reason; one cannot write a spin wave in terms of distortions of the parameters $\{a_i, b_i\}$. The spinwaves are non-analytic distortions of the BP Skymions. For example, in the zero charge sector the BP solution is simply the ferromagnetic ground state and does not allow for spin waves.

Including dynamical terms, the action for Skymions in the quantum Hall effect is¹

$$S = \int d^2x dt \frac{\nu \bar{\rho}}{2} \mathbf{A}[\mathbf{n}(\mathbf{r})] \cdot \frac{\partial \mathbf{n}}{\partial t} - \int dt E, \quad (51)$$

where E is given by Eq.(1) and $\mathbf{A}[\mathbf{n}(\mathbf{r})]$ is the vector potential of a unit monopole in spin space. Ignoring the Coulomb interaction, this gives the following equation of motion for spin waves^{16,17}:

$$\frac{\nu \bar{\rho}}{2} \frac{\partial \mathbf{n}}{\partial t} = \rho_s \mathbf{n} \times \nabla^2 \mathbf{n} + \bar{\rho} g_L \mathbf{n} \times \mathbf{B}. \quad (52)$$

These are known as the Lifshitz equations. For small Skymions, we expect essentially the same spin wave dispersion as for the ferromagnetic groundstate. In fact, on large length scales, the spin distribution looks like a ferromagnet, aside from at isolated points where the Skymions lie. The spectrum is,

$$\omega(\mathbf{k}) = \frac{2}{\nu \bar{\rho}} (\rho_s |\mathbf{k}|^2 + \bar{\rho} g_L B). \quad (53)$$

In addition to the gapped ferromagnetic spin wave, there is an anti-ferromagnetic mode with a linear spectrum, associated with the anti-ferromagnetic order of the in plane components of the spin distribution¹⁸. In principle one may calculate the spectrum of this mode by coarse graining the action for small fluctuations about the Skymion crystal on a lattice with half the period of the Skymion crystal. Staggering the effective action on this lattice, taking the continuum limit and integrating out the fast modes will give an effective action for the anti-ferromagnetic fluctuations. The solution of this problem is extremely complicated and depends on all the parameters of the system in a complicated way through the ground state configuration. In any case, our primary goal is to discuss the melting of the Skymion lattice, a process which is unaffected by the presence of spin waves.

Including the Coulomb interaction will cause a mixing between these spin waves and the Wigner crystal modes determined above. It is difficult to estimate this mixing and we will assume it to be negligible.

VIII. MELTING OF THE SKYRME CRYSTAL.

There are three steps in our analysis of the melting of the Skymion crystal: Firstly, we discuss the regime in which quantum fluctuations may be neglected. Next, we describe the various possibilities for defect mediated melting of the crystal and compare the predictions with experiment. Finally, we estimate at what temperature significant fluctuations in the size of the Skymions are to be expected.

A. Quantum Fluctuations.

In the usual way, quantum fluctuations of a particular mode may be neglected if the temperature is sufficiently high that the first Matsubara frequency, $2\pi T$, is larger than the energy of the mode at the momentum cut-off. With a high momentum cut-off at the first Brillouin zone, $|\mathbf{k}_{max}|^2 = \pi^2/a_0^2 = \sqrt{3}\pi^2 \bar{q}/2$, using the phonon dispersion from Eq.(50) and substituting the expressions for \mathcal{L} and \mathcal{T} from Eq.(25), we obtain the condition,

$$T \gtrsim 0.03 \frac{(e\nu_0)^2}{\epsilon l} |\nu/\nu_0 - 1|^{3/2} \sim 5 |\nu/\nu_0 - 1|^{3/2} K, \quad (54)$$

for the temperature above which quantum fluctuations of the phonon mode may be neglected. As indicated, for experimental values of the parameters this temperature is only a few tenths of a Kelvin. A similar analysis for spinwaves performed in Ref.[6] gives the following estimate for the temperature above which these quantum fluctuations can be neglected:

$$T \gtrsim \frac{2\rho_s}{\nu^2} |\nu/\nu_0 - 1|, \quad (55)$$

which for $\nu_0 = 1$ gives the temperature of order of $10|\nu/\nu_0 - 1|K$. If conditions (54, 55) are satisfied, the Skyrmion crystal becomes an entirely classical object. In fact it can be called a crystal only in a loose sense. Since the second derivatives of energy are proportional to $|\mathbf{k}|^2$, the fluctuations of displacements diverge logarithmically :

$$\langle u^2 \rangle = \frac{V_c T}{(2\pi)^2} \int \frac{d^2 k}{T|\mathbf{k}|^2} \sim \frac{V_c T}{T} \ln(L\sqrt{q}), \quad (56)$$

where L is the system size. In these circumstances, there is no long range positional order. As usual in two dimensions, however, one may have a finite stiffness, $T \neq 0$ which is associated with a directional long range order.

B. 2-Dimensional Melting.

The melting transition in two dimensions is driven by the presence of defects; dislocations and disclinations¹⁹. First attempts at explaining the melting transition treated these two types of defect as independent. The resulting system displays two second order Kosterlitz-Thouless type transitions, as first the dislocations and then the disclinations unbind with increasing temperature. At the dislocation unbinding transition we pass from the crystal phase, with long range directional order and power law decay of positional order, to a liquid crystal phase which has exponential decay of positional order and a power law decay of orientational order, (for an underlying hexagonal symmetry, this phase is known as a hexatic). The second transition is from the hexatic to an isotropic liquid which has exponential decays in both positional and orientational order. This picture, the Kosterlitz-Thouless-Nelson-Halperin-Young (KTNHY)²⁰ model, has several successes. Allowing for renormalisations of the elasticities due to the presence of phonons and dislocations, the lower temperature transition from the solid to the hexatic phase occurs at the same temperature as seen in some experimental systems, (notably the electronic Wigner crystal), and numerical simulations. Unfortunately, this is not the full story. Even those melting transitions whose temperatures are predicted correctly show some characteristics of being first order. Singularities in specific heat are always too sharp to be adequately described by a Kosterlitz-Thouless type transition.

A mechanism by which defect mediated melting in two dimensions could be first order was pointed out by Kleinert²¹. He noted that in fact dislocations and disclinations are not independent. A dislocation can be viewed as a bound pair of disclinations and a disclination as a string of dislocations. Although the formation of an isolated disclination has an enormous cost in strain energy, this is screened by the presence of dislocations. In fact the dislocation density acts like an effective temperature for the disclinations, and virtual fluctuations can lead to a Kosterlitz-Thouless transition at which disclinations proliferate. The presence of disclinations also modifies the effective potential of the dislocation density, which develops a second minimum at some non-zero density of dislocations. For a certain temperature this minimum is at zero energy and the feedback between the dislocations and disclinations drives a first order transition directly to the liquid. This occurs at a temperature below the Kosterlitz-Thouless transition temperature. This picture is still only a caricature of the actual melting process. In fact, dislocations need not pile up on neighbouring sites to form a disclination. If dislocations form a string along next nearest neighbour sites, the resulting configuration is identical to a grain boundary and the transition may be driven first order by a proliferation of these boundaries. It is sufficient that one allows for the possibility of dislocations forming strings by not choosing a prohibitive form of the core energy²¹.

The question remains which of these models is applicable to a particular system. A lattice model of defects demonstrating all of these features has been presented by Kleinert²². Whether the melting proceeds via two second order transitions or a single first order transition depends upon the length scale of local rotational stiffness. The following partition function describes a lattice with dislocation and disclination defects:

$$Z = \prod_x \left(\int_{-\pi}^{\pi} du_i(x) \right) \sum_{\{n_{ij}(x), m_i(x)\}} \exp(-\beta E),$$

$$E = \frac{1}{4} \sum_{x, ij} (\nabla_i u_i + \nabla_j u_i - 2\pi n_{ij})^2 + \frac{2\lambda}{\mu} \sum_{x, i} (\nabla_i u_i - \pi n_{ii})^2 + \frac{2l^2}{a^2} \sum_{x, i} (\nabla_i w - 2\pi m_i)^2 \quad (57)$$

The particles are placed at the sites of a simple square lattice with sites labeled, x . Derivatives are all lattice derivatives; $\nabla f(x) = f(x+i) - f(x)$, $\bar{\nabla}_i f(x) = f(x) - f(x-i)$. $u_i(x)$ is the displacement in the i direction of the particle at site x , normalised so that when $u_i = 2\pi$, the atom has been displaced by one lattice period, a . The inverse

temperature is, $\beta = a^2\mu/(2\pi)^2T$. With this normalisation, λ and $\mu = TV_c/2$ are the usual Lamé elastic constants. For future reference, we define the Poisson ratio as, $\tilde{\nu} = \lambda/(\lambda + 2\mu)$. Summations over integer n_{ij} and even n_{ii} allow for periodic jumps of atoms to neighbouring sites. This models the presence of dislocations. In the absence of dislocations, the first two terms appearing in the energy functional are simply the energy given by linear elasticity theory. The presence of disclinations is accounted for by the third term. Disclinations are very singular objects which cause large distortions of the lattice. In the vicinity of the disclination linear elasticity theory breaks down, and one must include a term which is proportional to the square of the local rotation field, $w = (\nabla_1 u_2 - \nabla_2 u_1)/2$. l characterises the length scale over which the lattice is stiff to local rotations.

One final point is that the sum over n_{ij} is unconstrained so that in effect atoms can hop onto neighbouring sites with no energy cost. For molecular or electronic crystals, one must modify the theory to allow for the singular repulsion between particles. For the Skyrme crystal, this is not necessary since two Skyrmions may easily sit on top of one another to form a doubly charged Skyrmion.

A dual representation of this model in terms of stress gauge fields, may be obtained, by introducing the stress tensor, σ_{ij} , and the rotational stress tensor, τ_i , via a Gaussian transformation and then integrating out the strain fields, $u_i(x)$ and $w(x)$. The stress gauge fields are defined in terms of the stress tensors as, $\sigma_{ij} = \epsilon_{ij}\bar{\nabla}_k A_k$, $\tau_i = \epsilon_{ij}\bar{\nabla}_j h - A_i$. In terms of these, the energy functional takes the form,

$$\beta E = \sum_x \left\{ \frac{1}{4\beta} \left[\frac{1}{1+\tilde{\nu}} (\nabla_i A_j)^2 - \frac{1}{2} \frac{1-\tilde{\nu}}{1+\tilde{\nu}} (\bar{\nabla}_i A_i)^2 \right] + \frac{a^2}{8\beta l^2} (\bar{\nabla}_k h - \epsilon_{kl} A_l)^2 - 2\pi i (A_i \bar{b}_i + h \bar{\theta}) \right\}, \quad (58)$$

where $\bar{b}_i = \epsilon_{jk}\nabla_j n_{ki} - m_i$ and $\bar{\theta} = \epsilon_{ki}\nabla_k m_i$ are the integer valued dislocation and disclination densities respectively.

This partition function may be written purely in terms of the defect fields, \bar{b}_i and $\bar{\theta}$, by integrating out the stress gauge fields, A_i and h . From Eq.(58), the effective partition function in its pure defect form is,

$$Z = \sum_{\{\bar{b}_i(x)\}} \exp - \left[4\pi^2\beta(\tilde{\nu} + 1) \sum_x \epsilon_{ij}\nabla_i \bar{b}_j(x) (-\bar{\nabla}\cdot\nabla)^{-1} \epsilon_{kl}\nabla_l \bar{b}_k(x) + 8\pi^2\beta \sum_x \nabla_i \bar{b}_i(x) \left\{ -\bar{\nabla}\cdot\nabla \left(\frac{a^2}{l^2} - \bar{\nabla}\cdot\nabla \right) \right\}^{-1} \nabla_j \bar{b}_j(x) \right]. \quad (59)$$

The character of the phase transitions in this model depend strongly upon the length scale of rotational stiffness. For very large l the KTHNY picture holds and there are two continuous transitions. For infinite l and $\tilde{\nu} = 1$, the partition function reduces to,

$$Z = \sum_{\{\bar{b}_i(x)\}} \exp \left[-8\pi^2\beta \sum_x \bar{b}_i(x) (-\bar{\nabla}\cdot\nabla)^{-1} \bar{b}_i(x) \right], \quad (60)$$

which has a Kostelitz-Thouless type phase transition at $4\beta = 2/\pi$. For very large but finite l , the longitudinal part of the field \bar{b} , is massive and does not contribute to the critical behaviour. The remaining contribution, from the transverse component, is given by the first term in the exponent of Eq.(59). This may be written,

$$Z = \sum_{\{\bar{b}_i(x)\}} \exp \left[-4\pi^2\beta(\tilde{\nu} + 1) \sum_x \bar{b}_i(x) \frac{\delta_{ij}\bar{\nabla}\cdot\nabla - \nabla_i\bar{\nabla}_j}{(\bar{\nabla}\cdot\nabla)^2} \bar{b}_j(x) \right]. \quad (61)$$

The long range form of the effective potential between the dislocations, is given by,

$$\frac{\delta_{ij}\bar{\nabla}\cdot\nabla - \nabla_i\bar{\nabla}_j}{(\bar{\nabla}\cdot\nabla)^2} \rightarrow \lim_{\delta \rightarrow 0} \int \frac{d^2q}{(2\pi)^2} \frac{e^{i\mathbf{q}\cdot\mathbf{x}}}{(q^2 + \delta^2)^2} (\delta_{ij}q^2 - q_i q_j) \approx \frac{1}{4\pi} \left(\delta_{ij} \ln|x| - \frac{x_i x_j}{|x|^2} \right). \quad (62)$$

We have used differentials of the series expansions of the zeroth order Bessel function in order to obtain this results. The pairwise interaction energy of the dislocations is, $E_{int} = 2\pi\beta(1+\tilde{\nu}) \ln|x|$, and there is an unbinding transition at a temperature, $(1+\tilde{\nu})\beta = 2/\pi$, or, $T = a^2\mu(1+\tilde{\nu})/8\pi$. This is the universal temperature for the dislocation unbinding transition, predicted by KTHNY. In Ref.[23], Morf calculated the renormalisation of the elastic constant, μ , for the electronic Wigner crystal at finite temperature, due to the presence of phonons and dislocations. With a suitable rescaling of the parameters, this result may be applied directly to the Skyrmion crystal. The melting temperature, allowing for this renormalisation, is

$$T_m = |\nu/\nu_0 - 1|^{1/2} \frac{(e\nu_0)^2}{\epsilon l} \frac{1}{2 \times 128.2\sqrt{2}} \simeq 0.44|\nu/\nu_0 - 1|^{1/2}. \quad (63)$$

For small $\beta \approx a^2/l^2$, the effective partition function is,

$$Z = \sum_{\{\bar{\theta}(x)\}} \exp \left(2 \frac{l^2}{a^2} 4\pi^2 \beta \sum_x \bar{\theta}(x) (-\bar{\nabla} \cdot \nabla)^{-1} \bar{\theta}(x) \right). \quad (64)$$

This model is equivalent to a Coulomb gas and has a KT transition at $4\beta l^2/a^2 \approx 2/\pi$, where the disclinations unbind.

For very small l , there is a single first order phase transition. The constraint $\bar{\nabla}_k h = \epsilon_{kl} A_l$ is forced upon the stress gauge fields, (see Eq.(58)). The energy functional then becomes,

$$\beta E = \sum_x \left[\frac{1}{4\beta(1+\tilde{\nu})} (\nabla \bar{\nabla} h)^2 + 2\pi i (\bar{b}_i \epsilon_{ij} \bar{\nabla}_i h + \bar{\theta} h) \right]. \quad (65)$$

This model shows a single first order phase transition at $(1+\tilde{\nu})\beta = 0.941$. If one studies the same transition in the model in which quadratic terms in the original energy functional, Eq.(57), are replaced by cosines, the predicted temperature is, $(1+\tilde{\nu})\beta = 1.328$. Not allowing for renormalisation of the elastic constants at finite temperature, *i.e.* setting μ and $\tilde{\nu}$ to their zero temperature values, we obtain the following prediction for the melting temperature:

$$T_m = \frac{(1+\tilde{\nu})}{1.328} \frac{a^2 \mu}{(2\pi)^2} = 0.48|\nu/\nu_0 - 1|^{1/2}. \quad (66)$$

Allowing for the renormalisation of μ by phonons at finite temperature, ($\tilde{\nu}$ remains virtually unchanged), this temperature is reduced to $T_m = 0.38|\nu/\nu_0 - 1|^{1/2}$. For the cosine model the corresponding temperature is, $T_m = 0.34|\nu/\nu_0 - 1|^{1/2}$ without renormalisation and $T_m = 0.27|\nu/\nu_0 - 1|^{1/2}$ with²⁴. Figure 3 shows a sketch of the way in which the renormalisation curve for μ calculated by Morf²³ is used to obtain these corrections to the transition temperatures. there will of course be additional renormalisation of the elastic constant which we have not allowed for here, due to the presence defects.

At some intermediate value of l , there is a change from the first order transition to two second order transitions. On the basis of numerical simulations to determine the position of this change over, Kleinert has predicted²⁵ that the Wigner crystal should undergo a first order transition. The actual value of l for the Wigner crystal lies very close to the change over, and so the transition is nearly continuous. We expect that since the Skyrmion crystal shares the same phonon spectrum as the Wigner crystal, it too should undergo a first order melting transition.

C. Comparison with Experiment.

Recent experimental measurements of the heat capacity of a two dimensional electron system in the quantum Hall regime, made by Bayot *et al.*²⁶ show a marked peak at a temperature of around $40mK$ with a deviation from total filling $\nu_0 = 1$ of around $|\nu/\nu_0 - 1| \sim 0.2$. These authors argue that this contribution to the specific heat comes from coupling of the nuclear spins to the Skyrmion spin distribution and that the sharp peak indicates a melting of the Skyrmion lattice. The sharpness of the peak suggests a first order transition, which accords with our prediction based on the criterion for the local rotational stiffness. The temperature of the first order transition in our lattice defect model is a factor of three or so greater than the experimental value at $|\nu/\nu_0 - 1| \sim 0.2$. There are two points to note in reconciling this difference: (i.) $|\nu/\nu_0 - 1| = 0.2$ is actually outside the regime where quantum fluctuations of phonons can be neglected at the melting point. These fluctuations may lead to a reduction in the melting temperature. (ii.) Softening of the pairwise interaction between Skyrmions as they begin to overlap means that in regions of large distortion such as near a defect, the effective lattice stiffness is reduced and the melting temperature is lowered accordingly.

This latter point may be better seen by comparing our partition function with that for an N-body system with a pairwise interaction potential, $\Phi(x-y)$ ²⁷. The partition function is,

$$Z = \int \frac{dx_1 \dots dx_N}{N!} \exp \left[-\frac{\beta}{2} \sum_{i \neq j} \Phi(\mathbf{x}_i - \mathbf{x}_j) \right]. \quad (67)$$

We consider a crystalline state at low temperature, where the particles fluctuate around lattice sites, \mathbf{x} , with small displacements, \mathbf{u} . the partition function may then be written as,

$$Z = \frac{1}{N!} \sum_{x,i} \prod_{x,i} \left(\int_{-\infty}^{\infty} du_i(\mathbf{x}) \right) \exp \left[-\frac{\beta}{2} \sum_{x \neq y} \Phi(\mathbf{x} - \mathbf{y} + \mathbf{u}(\mathbf{x}) - \mathbf{u}(\mathbf{y})) \right]. \quad (68)$$

Taylor expanding the partition function about the equilibrium configuration,

$$Z = \frac{1}{N!} \sum_{x,i} \prod_{x,i} \left(\int_{-\infty}^{\infty} du_i(\mathbf{x}) \right) \exp \left[-\frac{\beta}{4} \sum_{x \neq y} \partial_i \partial_j \Phi(x-y) (x-y)_k (x-y)_l \nabla_k u_i(x) \nabla_l u_j(y) \right]. \quad (69)$$

For equilibrium configurations including defects, the lattice gradients $\nabla_i u_j$ are no longer zero, but equal to the jump numbers, n_{ij} . Therefore, we make a similar Taylor expansion in powers of $\nabla_i u_j - n_{ij}$. It is obvious from this final form of the partition function and by comparison with Eq.(57) that a reduction in the curvature of the pair interaction potential effectively reduces the elastic constant. In going from the Villain, (quadratic), approximation to the cosine approximation for the elastic energy, the non-linearities in the cosine allow for such a reduction in the elastic constant, hence the lower melting temperature.

We conclude that the peak in heat capacity seen by Bayot *et al.* is consistent with a first order defect mediated melting of the Skyrmion lattice to a liquid of equal sized Skyrmions. Up to $|\nu/\nu_0 - 1| \sim 0.05$, the melting temperature is expected to vary as $|\nu/\nu_0 - 1|^{1/2}$. Beyond this quantum fluctuations are important and the melting is no longer classical. We sketch this behaviour in figure 4.

D. Fluctuations in the Skyrmion size.

Now we discuss the criteria for fluctuations in the size of the Skyrmions to be important. The mean square size of these fluctuations is

$$\langle u^2 \rangle = \frac{V_c T}{8\delta} \int \frac{|\mathbf{k}|^2 d^2 k}{(2\pi)^2} \sim \frac{V_c T |\mathbf{k}_{max}|^4}{64\pi\delta}. \quad (70)$$

To estimate when these fluctuations are significant, we use a Lindeman criterion; $\langle u^2 \rangle / V_c \sim 1$. This is satisfied for temperatures greater than

$$T \gtrsim \frac{128}{\pi^3} \frac{(\epsilon\nu_0)^2}{\epsilon l} |\nu/\nu_0 - 1|^{1/2} \left(\frac{-2 \ln \alpha}{3\alpha} \right)^{1/3} \sim 700 |\nu/\nu_0 - 1|^{1/2} \left(\frac{-2 \ln \alpha}{3\alpha} \right)^{1/3} K. \quad (71)$$

This temperature is always several thousand times the melting temperature and in the experimental range of parameters with $|\nu/\nu_0 - 1| \sim 0.2$ is around $300K$. In fact to achieve a realistic temperature for this transition, say of the order of $1K$, would require a reduction in the effective Zeeman coupling by a factor of ~ 100 . This takes us outside of the regime where our approximations are self-consistent and so we must be cautious about such assertions. However, we may be certain that no such fluctuations in the size of Skyrmions occur in the experimental range of parameters and that the transition to the meron liquid described in Ref.[6] does not occur.

At temperatures of around $4\pi\rho_s$ significant thermal excitation of Skyrmion anti-Skyrmion pairs will begin to occur, and our restriction to distorted BP solutions will be inadequate.

IX. SUMMARY.

At moderate Zeeman energies, the distortion of Skyrmions in the fractional quantum Hall effect is small and one may describe spin textures using the Belavin-Polyakov solutions. We show that there is a range of parameters where one may self-consistently assume that the charge density of the spin distribution occurs at isolated points. This range is spanned by that realised experimentally. The spin distribution of many Skyrmions depends in a very non-local way upon the Skyrmion coordinates. However, the interplay of Coulomb and Zeeman energies is such that near the classical minimum the behaviour accords with the intuitive picture of equal sized Skyrmions interacting via a residual point-like Coulomb interaction. At low temperatures these form a Wigner crystal with hexagonal symmetry. When one takes note of the azimuthal components of the spin texture, the full hexagonal symmetry is no longer apparent; the Skyrmions form a face centred rectangular lattice with sides close to the ratio $1 : \sqrt{3}$. The analytic expression for this distribution is given by $w = h\alpha(z, e^{2\pi i/3})$. In fact, accounting for the higher moments in the Coulomb interaction, the actual symmetry is expected to be rectangular with sides in a ratio somewhere between $1 : \sqrt{3}$ and $1 : 1$.

The phonon spectrum of the Skyrmion crystal has four modes. Two of these correspond to the phonon modes of the electronic Wigner crystal and two extremely stiff modes correspond to fluctuations in the size of the Skyrmions. Quantum fluctuations of these modes may be neglected for filling fractions close enough to $\nu_0 = 1$ and for a sufficiently high temperature. We have investigated the defect mediated melting of the Skyrmion crystal in this classical regime. A first order transition is predicted which is consistent with recent experiment. Fluctuations of the size of Skyrmions and the transition to a meron liquid requires a huge decrease in the effective Zeeman coupling and is not expected in the experimental range of parameters.

X. ACKNOWLEDGEMENTS.

We would like to thank J. Chalker and A. Rutenberg for helpful discussions and for their interest in the work.

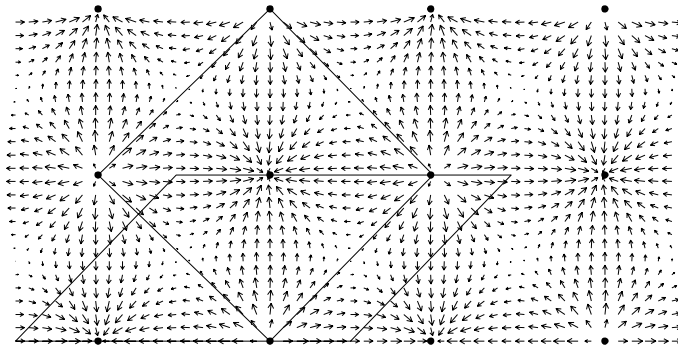


FIG. 1. **Square Skyrmion Lattice:** plot of (n_x, n_y) derived from $w(z) = h \sigma(z, 1/\sqrt{2})$. The dots indicate the zeros of the function $w(z)$. The square cell is that chosen by Brey et al. and the parallelepiped is the standard cell.

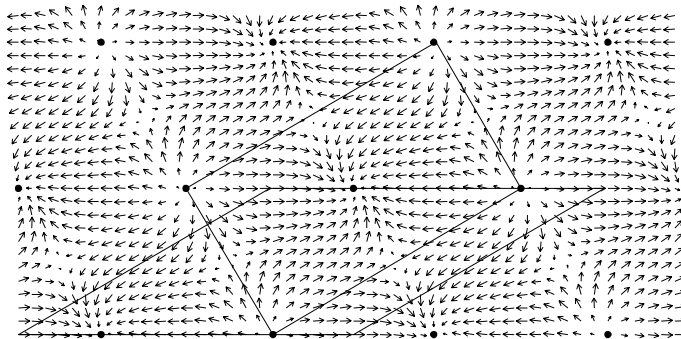


FIG. 2. **Hexagonal Skyrmion Lattice:** plot of (n_x, n_y) derived from $w(z) = h \sigma(z, e^{i2\pi/3})$. The dots indicate the zeros of the function $w(z)$. The solid lines indicate the standard cell and the face centred rectangular cell.

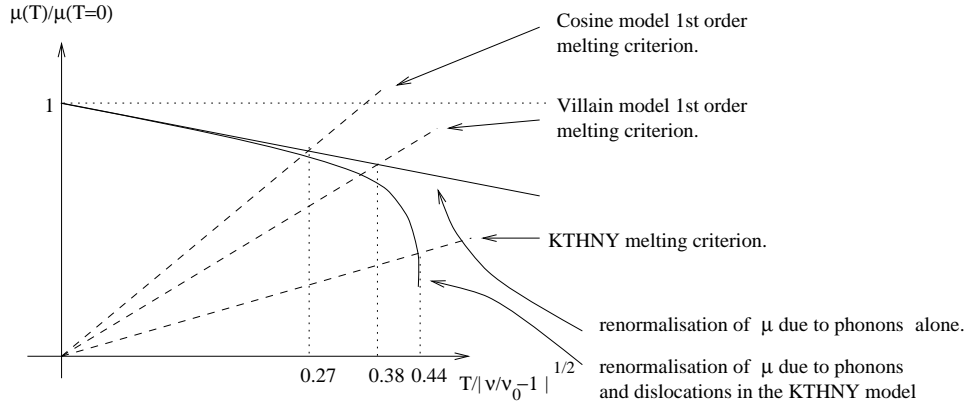


FIG. 3. **RG flow of elasticity:** The solid curve shows the finite temperature renormalisation of the elastic constant μ due to the presence of phonons and dislocations. The straight dashed lines show the various melting criteria. The points of intersection between the RG curve and the melting criteria give the melting points. Intersections with the horizontal dotted line at $\mu(T)/\mu(0)$ give the melting points without renormalisation corrections. see Ref.[23]

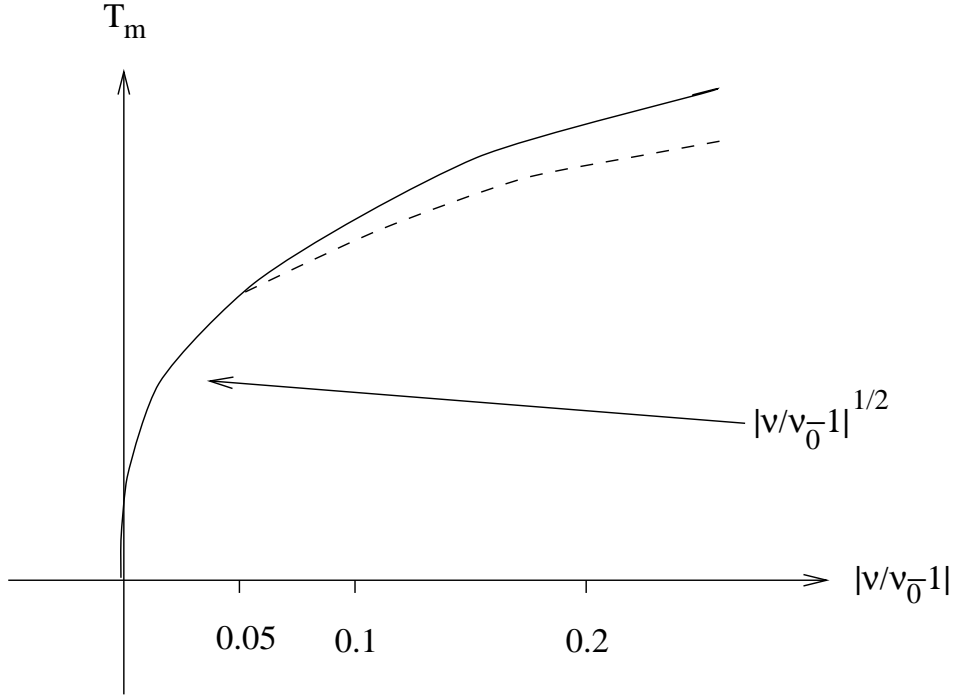


FIG. 4. **Predicted melting temperature versus $|\nu/\nu_0 - 1|$:** Up to $|\nu/\nu_0 - 1| \sim 0.05$ the system is classical up to the melting temperature and we expect $T_M \sim |\nu/\nu_0 - 1|^{1/2}$. Beyond here quantum fluctuations may lower the melting temperature.

¹ S. L. Sondhi, A. Karlshede, S. A. Kivelson, and E. H. Rezayi, Phys. Rev. B **47**, 16 419 (1993).

² S. E. Barrett, G. Dabbagh, L. N. Pfeiferer, K. W. West, and R. Tycko, Phys. Rev. Lett. **74**, 5112 (1995); R. Tycko, S. E. Barrett, G. Dabbagh, L. N. Pfeiferer, and K. W. West, Science **268**, 1460 (1995).

³ E.H.Aifer, D.A.Broido, and B.B.Goldberg, Phys. Rev. Lett. **76**, 4, 680 (1996).

⁴ A. Schmeller, J. P. Eisenstein, L. N. Pfeiffer, and K. W. West, cond-matt 9606133, (1996)

- ⁵ V. A. Fateev, I. V. Frolov, and A. S. Schwarz, Nucl. Phys. B **154**, 1 (1979).
- ⁶ A.G.Green, I.I.Kogan, and A.M.Tselik Pys. Rev. B **53**, 12, 6981 (1996).
- ⁷ H. A. Fertig, L. Brey, R. Cote, and A. H. MacDonald, Phys. Rev. B **50**, 11 018 (1994).
- ⁸ L. Brey, H.A.Fertig, R. Cote, and A.H.MacDonald, Phys. Rev. Lett **75**, 13, 2562, (1995).
- ⁹ A. H. MacDonald, H. A. Fertig, and L. Brey, Phys. Rev. Lett. **76**,12,2153 (1996).
- ¹⁰ A. A. Belavin, and A. M. Polyakov, JETP Lett. **22**, 503 (1975).
- ¹¹ P.P. Ewald, Ann. Phys. (Leipz.) **54**, 519 (1917); **54**, 557 (1917); **64**, 263 (1921).
- ¹² L. Bonsall, and A.A. Maradudin, Phys. Rev. B **15**, 1959, (1977).
- ¹³ H. Fukuyama, Solid State Communications, **17**, 1323, (1975).
- ¹⁴ M. Stone, cond-matt 9512010 (1995).
- ¹⁵ J. Dziarmaga, cond-matt 9603124;
- ¹⁶ L. Landau, and E.M. Lifshitz, Statistical Physics, Pergamon, (1975).
- ¹⁷ M. Stone, Nuc. Phys. B **314**, 557 (1986)
- ¹⁸ In a recent preprint, the following authors have argued that the existence of ferromagnetic and anti-ferromagnetic modes is a very general property of such complicated spin distributions as we have here: S. Sachdev and T. Senthil, cond-matt 9602028 (1996).
- ¹⁹ H. Kleinert, Gauge Fields in Condensed Matter Physics Vol.2, World Scientific (1989).
- ²⁰ M. Kostelitz and D. J. Thouless, J. Phys. **C6**,1181 (1973). B. I. Halperin and D. R. Nelson, Phys. Rev. Lett. **41**, 2, 121 (1978); Phys. Rev Lett. **41**, 519 (1978); D. R. Nelson and B. I. Halperin, Phys. Rev. **B19**, 5, 2457 (1979); A. P. Young, Phys. Rev. **B19**, 1855 (1979).
- ²¹ H. Kleinert, Phys. Lett. A, **95A**, 7, 381 (1982); H. Kleinert, Phys. Lett. A, **95**, 9, 493 (1983); H. Kleinert, Lettre al nuovo cimento **37**, 8, 295 (1983); W. Janke, and H. Kleinert, Phys. Lett. A, **105**, 3, 134 (1984); W. Janke, and H. Kleinert, Phys. Rev. Lett. **61**, 20, 2344 (1988).
- ²² H. Kleinert, Phys. Lett. A, **130**, 8, 443 (1988); H. Kleinert, Phys. Lett. A, **9136**, 9, 468 (1989).
- ²³ R. H. Morf, Phys. Rev. Lett. **43**, 13, 931 (1979).
- ²⁴ In fact the melting temperature predicted for the Villain and cosine models on the square lattice are $(1 + \nu)\beta_m = 0.815$ and 1.15 respectively. The results for the triangular lattice are obtained by multiplying by an additional factor of $2/\sqrt{3}$. see Ch. 14.4 Ref.[19]
- ²⁵ H. Kleinert, Phys. Lett. A, **136**, 9, 468 (1989).
- ²⁶ V. Bayot, E. Grivei, S. Melinte, M. B. Santos and M. Shayegan, Phys. Rev. Lett. **76**, 3, 479 (1996).
- ²⁷ see Ch. 10.4 of Ref.[19].